ORIGINAL RESEARCH

Novel route synthesis of porous and solid gold nanoparticles for investigating their comparative performance as contrast agent in computed tomography scan and effect on liver and kidney function

Farooq Aziz[1,2]
Ayesha Ihsan[1]
Aalia Nazir[2]
Ishaq Ahmad[3]
Sadia Zafar Bajwa[1]
Asma Rehman[1]
Abdoulaye Diallo[4]
Waheed S Khan[1]

[1]Nanobiotechnology Group, National Institute for Biotechnology and Genetic Engineering (NIBGE), Faisalabad, [2]Department of Physics, Islamia University of Bahawalpur, Bahawalpur, [3]National Center for Physics, Quaid-I-Azam University, Islamabad, Pakistan; [4]Laboratory of Photonics and Nano-Fabrication, Faculty of Science and Technology, Cheikh Anta Diop University of Dakar (UCAD), Dakar-Fann Dakar, Senegal

Correspondence: Abdoulaye Diallo
Laboratory of Photonics and Nano-Fabrication, Faculty of Science and Technology, Cheikh Anta Diop University of Dakar (UCAD), BP 25114 Dakar-Fann Dakar, Senegal
Tel +221 33 837 0901
Email abdoulayediallosn@gmail.com

Waheed S Khan
Nanobiotechnology Group, National Institute for Biotechnology and Genetic Engineering (NIBGE), PO Box 577, Jhang Road, Faisalabad, Pakistan
Tel +92 41 920 1404
Fax +92 41 920 1322
Email waheedskhan@yahoo.com

Abstract: Gold nanoparticles (GNPs) with dimension in the range of 1–100 nm have a prominent role in a number of biomedical applications like imaging, drug delivery, and cancer therapy owing to their unique optical features and biocompatibility. In this work, we report a novel technique for the synthesis of two types of GNPs namely porous gold nanoparticles (PGNPs) and solid gold nanoparticles (SGNPs). PGNPs of size 35 nm were fabricated by reduction of gold (III) solution with lecithin followed by addition of L-ascorbic acid and tri-sodium citrate, whereas SGNPs with a dimension of 28 nm were prepared by reflux method using lecithin as a single reducing agent. Comparative studies using PGNPs (λ_{max} 560 nm) and SGNPs (λ_{max} 548 nm) were conducted for evaluating their use as a contrast agent. These studies reveled that in direct computed tomography scan, PGNPs exhibited brighter contrast (45 HU) than SGNPs (26 HU). To investigate the effect of PGNPs and SGNPs on the liver and kidney profile, male rabbits were intravenously injected with an equal dose of 1 mg/kg weight of PGNPs and SGNPs. The effect on biochemical parameters was evaluated 72 hours after intravenous (IV) injection including liver function profile, renal (kidney) function biomarker, random blood glucose value, and cholesterol level. During one comparison of contrast in CT scan, PGNPs showed significantly enhanced contrast in whole-rabbit and organ CT scan as compared to SGNPs 6 hours after injection. Our findings suggested that the novel PGNPs enhance CT scan image with higher efficacy as compared to SGNPs. The results showed that IV administration of synthesized PGNPs increases the levels of aspartate aminotransferase (AST), alkaline phosphate (ALP), serum creatinine, and blood glucose, whereas that of SGNPs increases the levels of AST, ALP, and blood glucose.

Keywords: porous gold nanoparticles, solid gold nanoparticles, CT scan, contrast agent, liver function test, renal function test

Introduction

Metal-based nanoparticles, in the size range of 1–100 nm, exhibit unique properties that are different from bulk and dissolved counterparts. In the medical field, nanoparticles have the potential to revolutionize diagnostics, drug delivery, and therapeutic and theranostic applications.[1–3] Applications of nanoparticles are diversified by the variability of size and their availabilities in many shapes, that is, nanorods,[4–6] nanoshells,[7–10] nanocages,[11,12] nanotriangles,[13] nanostars or dandrimers,[14–16] and nanocups.[17]

Among different inorganic nanoparticles, gold nanoparticles (GNPs) have been most studied due to their biocompatible nature and low-toxicity profile.[18,19] The surface of a nanoparticle may be smooth or rough. A smooth surface provides limited surface area as the size of nanoparticles is fixed. For a required dimension, a possible way to increase the surface area is to make nanoparticles with a rough or porous surface. These kinds of morphological features have a definite impact on the overall behavior of nanoparticles like physical constants (density and surface area), optical properties, and wetting.[20] These nanoscale features can also alter the biological interaction as the nanoparticle surface contacts the biological environment, and are a crucial determinant of the response; therefore, in addition to surface coating, surface charge, conjugated molecule, shape, and topography, the surface porosity/roughness may have enormous impact on the overall performance of nanoparticles like biodistribution, stability, target localization, cellular interaction, uptake, drug release, and toxicity. It has been reported earlier that the saturation uptake of biomolecules on roughened films increased by up to 70%, higher than the increase of surface area (20%).[21] Therefore, fine-tuning of nanoscale features is extremely important for effective bio-application of nanoparticles. Herein, we analyze the performance of solid and porous nanoparticles (having rough surface) as a computed tomography (CT) scan probe with a supposition that porous nanoparticles may have a better biodistribution and thus may function as a better contrast agent as compared to their solid counterpart.

CT scan has been widely used for noninvasive imaging and diagnosis of diseases.[22] It is a medical procedure in which X-rays are used to take cross-sectional images of the body to find abnormalities or presence of tumor when physical checkup is not possible. X-rays are passed through the patient's body and captured by the detectors. A three-dimensional image is formed on the basis of differential absorption of X-rays by tissues. The quality of image is important to reveal maximum possible information for the correct diagnosis and to evaluate the extent or stage of disease.[23] Image quality is proportional to X-ray dose and atomic number of different tissues. The X-ray attenuation in different tissues may range from −1,000 HU to 1,000 HU.[24] Traditionally, quality of image is improved by enhancing the dose of X-rays which may be toxic, especially when repeated imaging is advised in many diseases. Conventional CT contrast agents are based on small iodinated molecules. Despite their good efficiency for X-ray attenuation, these iodinated probes have short circulation time, nonspecific distribution, rapid pharmacokinetics, and nephrotoxicity. Due to these concerns, iodinated probes have limited usage for microvascular and targeting performance. Use of suitable nanoparticles can overcome these toxicity effects as well as may help to reduce the exposure of patients to X-rays. Due to their biocompatibility and higher atomic weight, GNPs have been much explored for theranostic applications. GNPs have been used as contrast agents for enhancing image quality due to high density and high atomic number. They can enhance X-ray attenuation and improve image quality.[25,26] One advantage of nanoparticles is their tunable colloidal stability which is helpful to improve the circulation time of nanoprobes. Owing to their high surface area and unique optical properties, rough-surfaced porous gold nanoparticles (PGNPs) and other anisotropic gold nanostructures are very alluring for use in theranostic imaging. However, application of these gold nanostructures has been limited by the complex manufacturing procedure, high cost, and toxicity due to surface ligands.[27] In this paper, we report a novel route for one-pot synthesis of solid gold nanoparticles (SGNPs) and PGNPs as CT contrast agents. Both SGNPs and PGNPs were prepared and stabilized with lecithin. Lecithin is a phospholipid which is well reported for its long circulation time, colloidal stability, and non-cytotoxicity.[28] The GNPs were compared with standard CT contrast, that is, iodine, for in vivo application (Figure 1).

Methods
Synthesis of PGNPs and SGNPs

Gold (III) chloride (99%; Thermo Fisher Scientific, Waltham, MA USA), lecithin granular (Thermo Fisher Scientific), L-ascorbic acid (99%; Bio Basic Inc., Markham, ON, Canada), and tri-sodium citrate (99.5%; Thermo Fisher Scientific) were used as starting materials throughout the study. All required glassware was washed with aqua regia and rinsed with distilled water before use.

For one-pot synthesis of PGNPs, an aqueous solution of gold salt ($AuCl_3$, 30 mL, 1 mM) was maintained at 50°C under stirring and then an aqueous solution of lecithin (4.5 mL, 20 mM) was added to it. Then, L-ascorbic acid (0.75 mL, 100 mM) was added under continuous stirring. Finally, tri-sodium citrate (0.75 mL, 100 mM) was added to this solution and stirred for 2 hours at 50°C. GNPs colloidal solution was centrifuged at 12,000 rpm for 20 minutes. Settled particles were collected and dispersed in water. The cleaning process was repeated three times with deionized water.

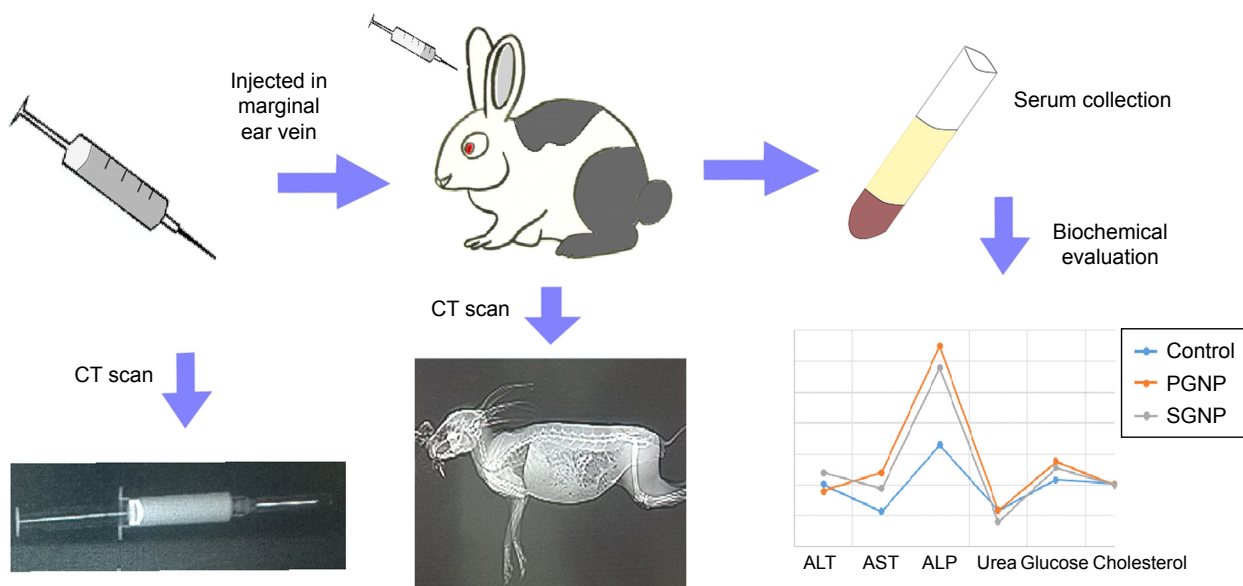SGNPs were prepared by one-step, one-pot reflux method. Aqueous solution of gold salt (1 mM, 30 mL) was

Figure 1 Process showing comparative performance of GNPs for contrast agent in CT scan and biochemical parameters.
Abbreviations: CT, computed tomography; PGNP, porous gold nanoparticle; SGNP, solid gold nanoparticle; ALT, alanine transferase; AST, aspartate aminotransferase; ALP, alkaline phosphate.

heated to 80°C under reflux, and aqueous solution of lecithin (10 mL, 10 mM) was added. The heated solution was stirred for 15 minutes. After cooling, SGNPs were washed thrice with deionized water as for PGNPs (Figure 2).

Characterization

The absorbance spectra of GNPs were measured by SpectraMax Plus 384 Microplate Reader. Hydrodynamic size and zeta potential of nanoparticles were determined by

Malvern Zetasizer (ZS90; Malvern Instruments, Malvern, UK). Field emission scanning electron microscope (FESEM, JSM 7500F; JEOL, Tokyo, Japan) at accelerating voltage (1–30 kV) was used to study the morphology of GNPs.

CT scans

PGNPs and SGNPs were evaluated in vitro for contrast properties in CT scan. A concentration of 20 mg/L of gold was taken to measure the density. For this purpose,
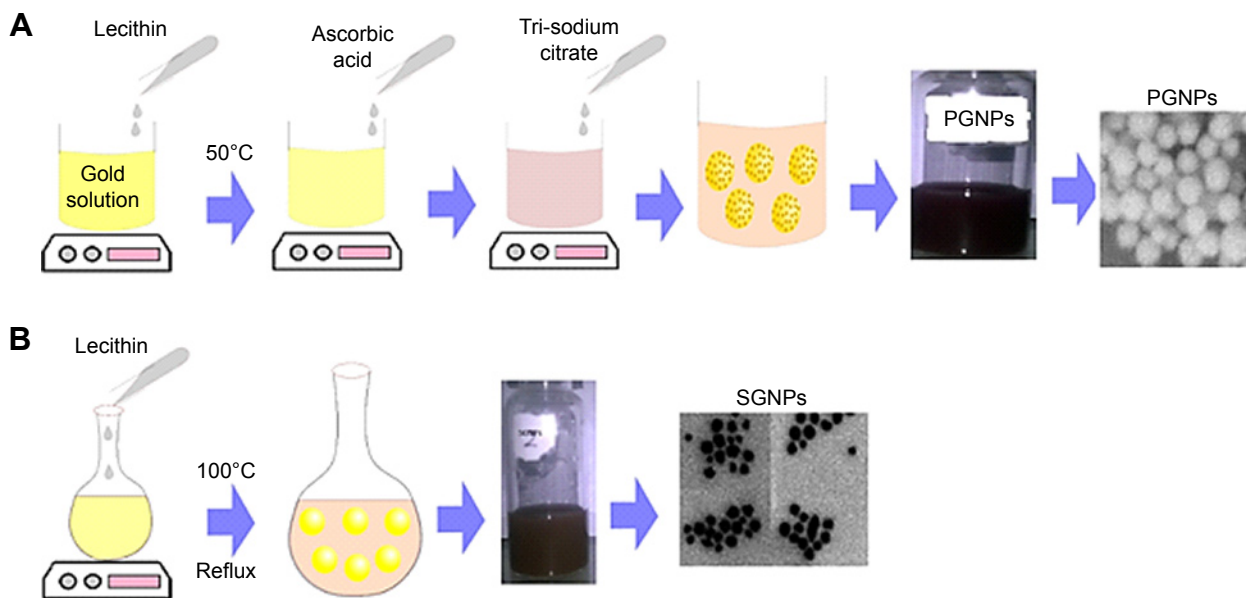

Figure 2 Schematic diagram of the synthesis of (**A**) PGNPs and (**B**) SGNPs.
Abbreviations: PGNPs, porous gold nanoparticles; SGNPs, solid gold nanoparticles.

PGNPs and SGNPs were taken in a syringe and imaged by Toshiba Aquilion CT scanner. Contrast efficiency of SGNPs and PGNPs was compared in terms of mean CT number expressed in Hounsfield units.

Animal studies

Procedures involving animals and their care were performed according to the guidelines prepared and approved by University of Veterinary and Animal Sciences, Lahore. These studies were approved by the Institutional Ethical Committee of NIBGE (Faisalabad, Pakistan). Six albino male rabbits were selected and divided into two groups. Group 1 was administered with PGNPs, and group 2 with SGNPs. One milligram of GNPs dispersed in 1 mL saline buffer was taken per 1 kg of body weight[29] and injected into the rabbits through the marginal ear vein. Blood samples were taken after 1, 2, and 3 days, and assays were performed for biochemical parameters of blood (serum glucose and cholesterol level), liver function (alanine transferase [ALT], alkaline phosphatase [ALP], aspartate aminotransferase [AST], bilirubin total), and renal function (blood urea and serum creatinine).

For in vivo imaging, two albino rabbits were injected with PGNPs and SGNPs equivalent to 1 mg of gold via the marginal ear vein. CT scan was taken after 6 hours of intravenous (IV) administration at a voltage of 120 kV, current of 250 mA, and total scan time of 6.741 seconds.

Results and discussion
Shape and surface morphology of NPs

The morphology of both kinds of gold particles was studied by scanning electron microscopy (SEM) and transmission electron microscopy (TEM). The samples for electron microscopic characterization were prepared by slow evaporation of a drop of an aqueous suspension of particles on carbon-coated copper grids. The SEM analysis of gold structures revealed granular shape, with an average size of 30–40 nm, having a rough surface comprising several nanostructured grains (Figure 3C). However, nanoparticles formed by using sole lecithin showed plain and solid surface (no pores; Figure 3A). The size range seemed to be 15–30 nm (Figure 3A). PGNPs showed a surface plasmon resonance (SPR) band at 560 nm, while the SGNPs showed an SPR band at 548 nm.
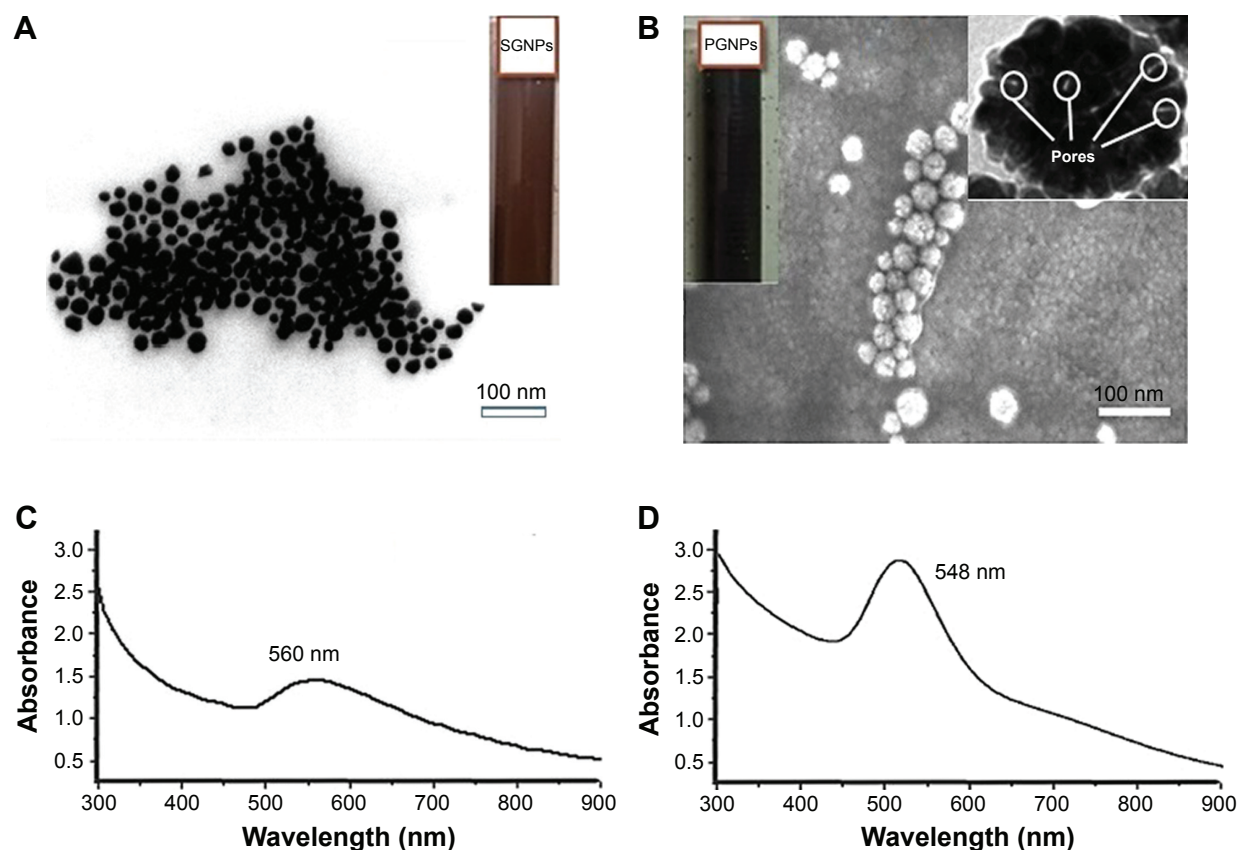

Figure 3 Characterization of SGNPs and PGNPs. (**A**) TEM image of SGNPs. (**B**) SEM image of PGNPs; pores on a single particle are labeled with white circles (inset). SPR spectrum of (**C**) PGNPs and (**D**) SGNPs.
Abbreviations: SGNPs, solid gold nanoparticles; PGNPs, porous gold nanoparticles; TEM, transmission electron microscopy; SEM, scanning electron microscopy; SPR, surface plasmon resonance.

Size and zeta potential

Hydrodynamic size of these GNPs was measured by dynamic light scattering (DLS; Zetasizer, ZS90; Malvern Instruments). Average DLS size of PGNPs and SGNPs was 35 nm and 28 nm, respectively (Figure 4A and B). This size range seemed suitable for IV injection and was reported for excellent biodistribution.[30] The zeta potential of PGNPs and SGNPs was −44.4 mV and −51 mV, which indicates excellent colloidal stability for both formulations.[31,32] The colloidal stability of these GNPs was further evaluated in different physiological media after 1 week. We found negligible change in nanoparticles size dispersed in water, phosphate-buffered saline solution, and Dulbecco's Modified Eagle's Medium indicating that nanoparticles are suitable for long-term use.

For initial screening of X-rays attenuation by PGNPs and SGNPs, direct scans of nanoparticles-containing syringes were taken (Figure 5). It has been reported in many studies that solid GNPs give around two to three times higher contrast than iodine, a commonly used contrast agent in CT scan.[33]

The results of our study showed that contrast efficiency of both PGNPs and SGNPs was in agreement with previous studies.[25,33,34] Interestingly, contrast efficiency of PGNPs was 1.73 times higher than SGNPs. These results suggest that both SGNPs and PGNPs may be preferred contrast agents in CT scan.

Previous studies have shown that GNPs injected into animal bodies get accumulated in the liver and kidneys, which could be lethal.[29,35] To examine the biocompatibility of PGNPs and SGNPs, their influence on blood biochemistry and liver and kidney function was studied in albino rabbits. All rabbits survived during the 3-day study period, and no change was observed in normal behavior, food intake, and
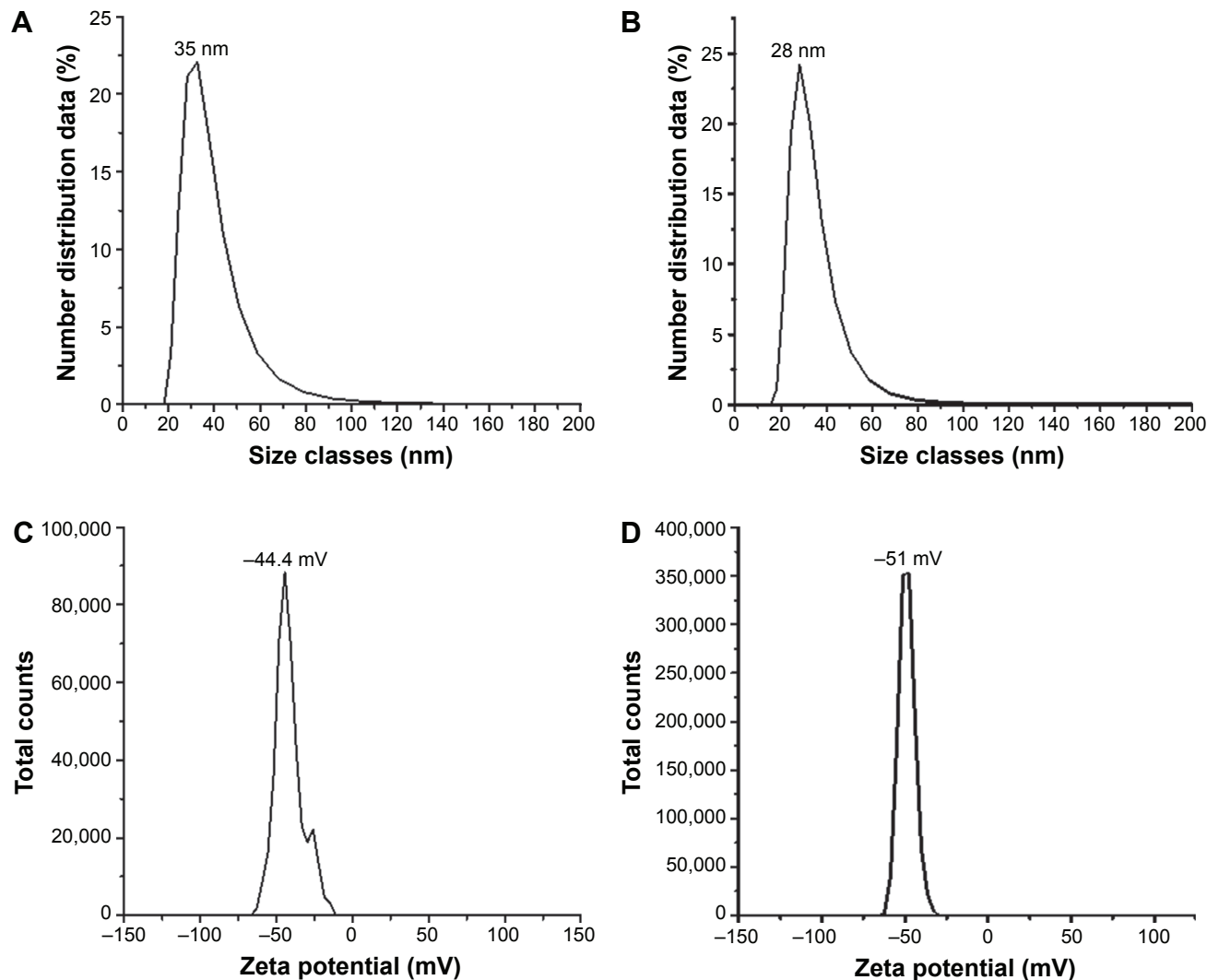

Figure 4 DLS study of nanoparticles: particle size of (**A**) PGNPs and (**B**) SGNPs; and zeta potential of (**C**) PGNPs and (**D**) SGNPs.
Abbreviations: DLS, dynamic light scattering; PGNPs, porous gold nanoparticles; SGNPs, solid gold nanoparticles.
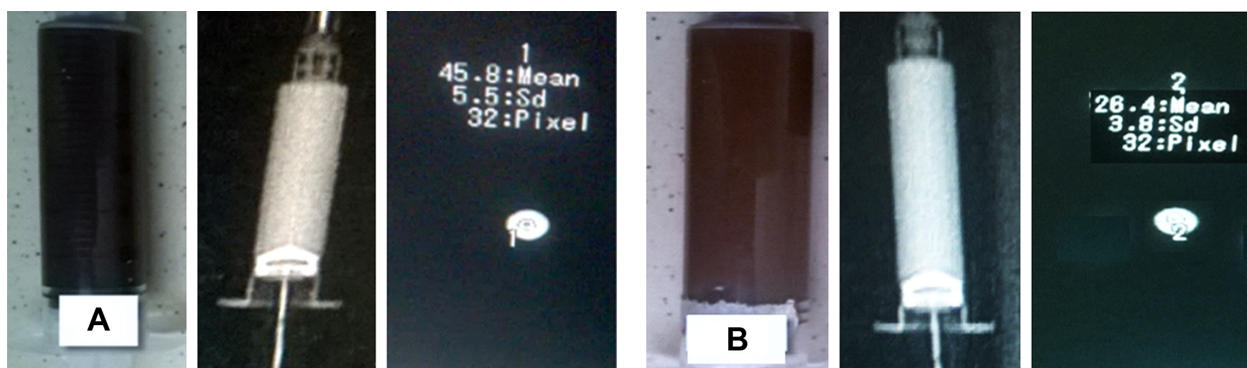
Figure 5 Direct CT scan image of (**A**) PGNPs and (**B**) SGNPs shows that porous shape has a better density value and thus better contrast display.
Abbreviations: CT, computed tomography; PGNPs, porous gold nanoparticles; SGNPs, solid gold nanoparticles.

physical function. The liver profile of animals after injection of nanoparticle formulation (PGNPs and SGNPs) showed a slight increase in the levels of ALT (Figure 6A), AST (Figure 6B), ALP (Figure 6C), and total bilirubin (Figure 6D). Data were collected for 3 days postinjection. Elevated levels of ALT and ASP in the first 2 days tended to get normalized on the 3rd day which indicates the lack of any kind of damage to the liver. Total bilirubin level remained almost constant for 2 days and increased slightly on the 3rd day in PGNP-administered rabbits. ALT is an enzyme that is found only in the liver, and bilirubin is a red blood cell component which is processed by the liver. Elevation of these blood markers indicates damage to hepatocytes. AST and ALP are found in the liver as well as other tissues and are routinely analyzed as liver function markers in combination with ALT and bilirubin. The kidney function is evaluated by measuring blood urea and creatinine that are cleared by the kidneys. Our results showed a slight decrease in the level of urea (Figure 6E) and creatinine (Figure 6F) after 3 days. By analyzing this data, we can say that kidney function is more influenced by PGNPs as compared to SGNPs. On the other hand, levels of blood glucose and cholesterol increase abruptly with both types of nanoparticles and tend to get normalized with time. These results suggest that both types of nanoparticles preliminarily accumulated in the liver and kidneys and interfered with their function which is in agreement with previous
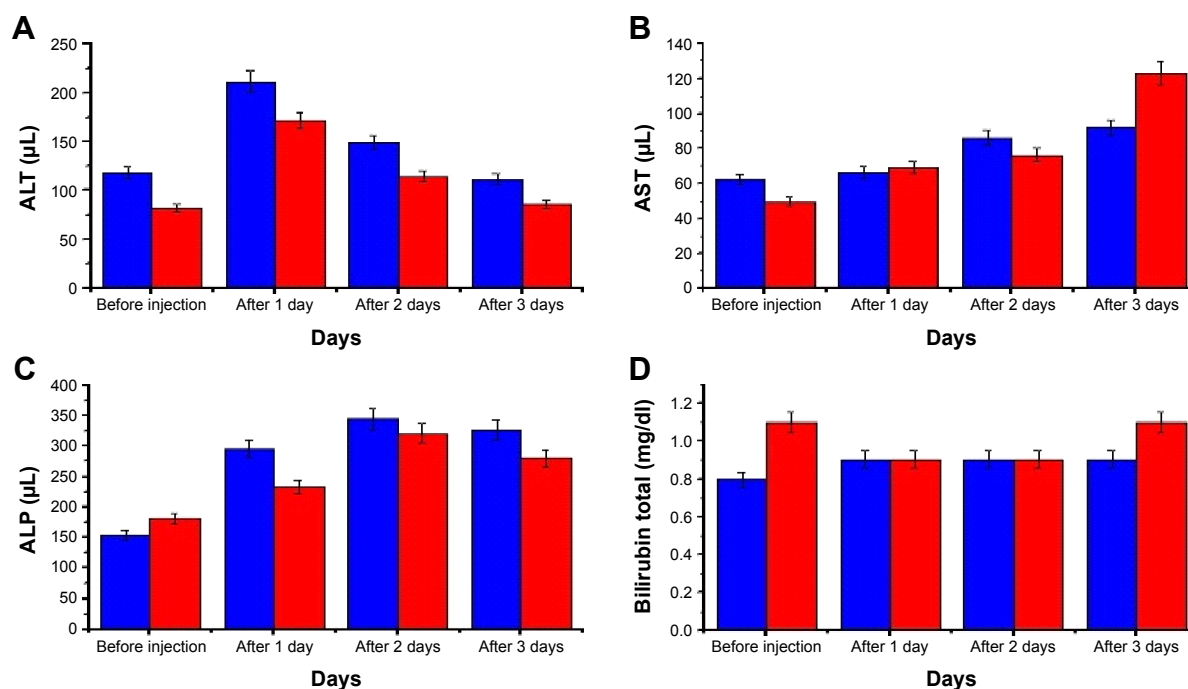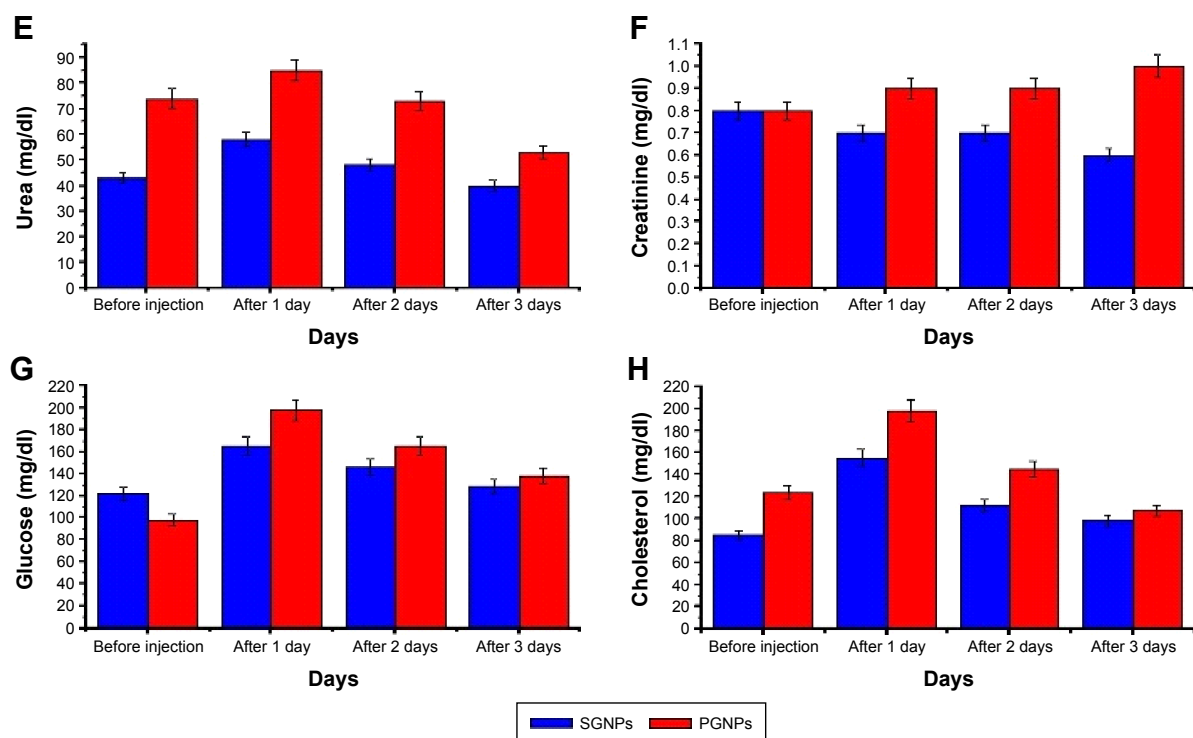

Figure 6 (*Continued*)

Figure 6 Biocompatibility of SGNPs (blue) and PGNPs (red) in rabbit. Influence on the value of (**A**) ALT, (**B**) AST, (**C**) ALP, (**D**) bilirubin total, (**E**) urea, (**F**) serum creatinine, (**G**) blood glucose, and (**H**) cholesterol.
Abbreviations: SGNPs, solid gold nanoparticles; PGNPs, porous gold nanoparticles; ALT, alanine transferase; AST, aspartate aminotransferase; ALP, alkaline phosphate.
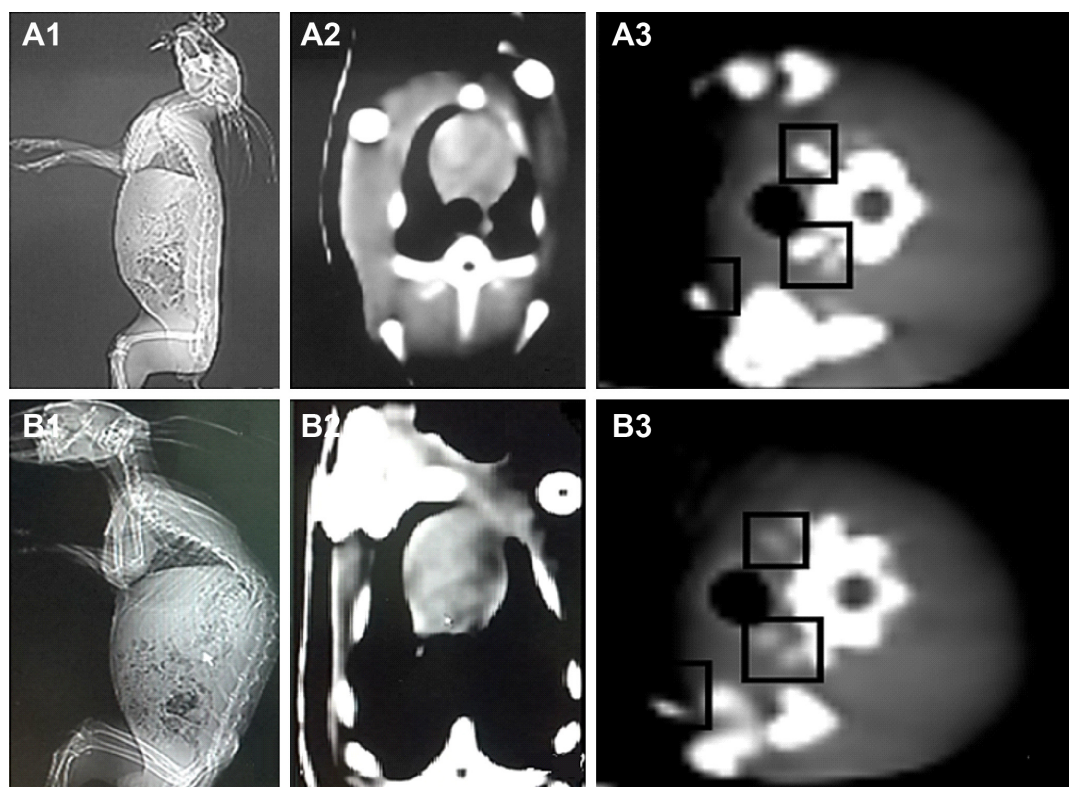

Figure 7 CT scan of rabbits treated with PGNPs and SGNPs. (**A1** and **A2**) Clear CT image obtained with PGNPs as contrast. (**A3**) Blur scan obtained with PGNPs as contrast. (**B1** and **B2**) Clear CT image obtained with SGNPs as contrast. (**B3**) Blur scans obtained with SGNPs as contrast.
Abbreviations: CT, computed tomography; SGNPs, solid gold nanoparticles; PGNPs, porous gold nanoparticles.

studies.[29,35] However, this effect seems to be reversible as both the kidneys and liver revert to their normal function after clearance of nanoparticles (Figure 6). Lack of toxicity has been broadly documented for negatively charged GNPs (probably due to their bare surface) in the size range reported in this paper and at a dose of 1 mg/kg.[27] Thus, it could be assumed that lecithin-coated PGNPs and SGNPs could be safely used in vivo as preferred contrast agents.

Two groups of rabbits were administered with PGNPs and SGNPS and evaluated by CT scan imaging (Figure 7). PGNPs showed superior contrast enhancement (Figure 7A1–A3) as compared to SGNPs (Figure 7B1–B3). These results are also supported by higher mean attenuation of PGNPs in vitro, as discussed. The manifold higher contrast efficiency of PGNPs was evident in full-body scan as well as organ-specific scan of rabbits suggesting that PGNPs synthesized by novel one-pot method can be used as safe and effective contrast agents in CT scan imaging.

Conclusion

In this work, we reported facile methods to synthesize PGNPs and SGNPs by using lecithin as a stabilizer. These nanoparticles could find vast application in imaging, and so in the present work, we compared 35 nm PGNPs and 28 nm SGNPs. These GNPs are stable at physiological conditions, and may have application in detection of localized tumors and thus may be useful for cancer imaging. To examine the contrast value of these nanoparticles in CT scan, both kinds of particles (porous and solid) were individually tested using the animal model. The results proved that PGNPs show better contrast due to their higher efficiency of X-rays attenuation, probably because of their rough or porous surface compared to SGNPs. SGNPs were observed to show blur contrast as compared to PGNPs. The biochemical impact of both GNPs was evaluated, by measuring the level of blood glucose, cholesterol, and liver and renal function biomarkers at different time intervals. Both SGNPs and PGNPs showed a pronounced effect on the liver function profile. The average values of blood urea and creatinine showed the minor effect of the GNPs on the renal profile. Based on this data, we can say with full confidence that PGNPs are more effective as CT scan probe, as compared to SGNPs and iodinated probe.

Acknowledgment

Disclosure

References

1. Ferrari M. Cancer nanotechnology: opportunities and challenges. *Nat Rev Cancer*. 2005;5(3):161–171.
2. Parveen S, Misra R, Sahoo SK. Nanoparticles: a boon to drug delivery, therapeutics, diagnostics and imaging. *Nanomedicine*. 2012; 8(2):147–166.
3. Bechet D, Couleaud P, Frochot C, Viriot ML, Guillemin F, Barberi-Heyob M. Nanoparticles as vehicles for delivery of photodynamic therapy agents. *Trends Biotechnol*. 2008;26(11):612–621.
4. Huff TB, Hansen MN, Zhao Y, Cheng JX, Wei A. Controlling the cellular uptake of gold nanorods. *Langmuir*. 2007;23(4):1596–1599.
5. Liao H, Hafner JH. Gold nanorod bioconjugates. *Chem Mater*. 2005; 17(18):4636–4641.
6. Niidome T, Yamagata M, Okamoto Y, et al. PEG-modified gold nanorods with a stealth character for in vivo applications. *J Control Release*. 2006;114(3):343–347.
7. Liu H, Chen D, Li L, et al. Multifunctional gold nanoshells on silica nanorattles: a platform for the combination of photothermal therapy and chemotherapy with low systemic toxicity. *Angew Chem*. 2011; 123(4):921–925.
8. Brongersma ML. Nanoscale photonics: nanoshells: gifts in a gold wrapper. *Nat Mater*. 2003;2(5):296–297.
9. Loo C, Lin A, Hirsch L, et al. Nanoshell-enabled photonics-based imaging and therapy of cancer. *Technol Cancer Res Treat*. 2004;3(1): 33–40.
10. Sounderya N, Zhang Y. Use of core/shell structured nanoparticles for biomedical applications. *Rec Patent Biomed Eng*. 2008;1(1): 34–42.
11. Skrabalak SE, Chen J, Au L, Lu X, Li X, Xia Y. Gold nanocages for biomedical applications. *Adv Mater*. 2007;19(20):3177–3184.
12. Hu M, Chen J, Li ZY, et al. Gold nanostructures: engineering their plasmonic properties for biomedical applications. *Chem Soc Rev*. 2006; 35(11):1084–1094.
13. Chu HC, Kuo CH, Huang MH. Thermal aqueous solution approach for the synthesis of triangular and hexagonal gold nanoplates with three different size ranges. *Inorg Chem*. 2006;45(2):808–813.
14. Guerrero-Martínez A, Barbosa S, Pastoriza-Santos I, Liz-Marzán LM. Nanostars shine bright for you: colloidal synthesis, properties and applications of branched metallic nanoparticles. *Curr Opin Colloid Interface Sci*. 2011;16(2):118–127.
15. Balogh LP, Minc LD, Berka M. Novel synthesis of radioactive gold/dendrimer composite nanoparticles for the treatment of cancer. *Nanomedicine: NBM*. 2007;3(4):351.
16. Owen DJ. Dendrimers: new opportunities to treat and prevent human diseases. *Nanomedicine: NBM*. 2007;3(4):338.
17. Ihsan A, Katsiev H, Alyami N, Anjum DH, Khan WS, Hussain I. From porous gold nanocups to porous nanospheres and solid particles–a new synthetic approach. *J Colloid Interface Sci*. 2015;446:59–66.
18. Nikoobakht B, El-Sayed MA. Preparation and growth mechanism of gold nanorods (NRs) using seed-mediated growth method. *Chem Mater*. 2003;15(10):1957–1962.
19. El-Sayed IH, Huang X, El-Sayed MA. Selective laser photo-thermal therapy of epithelial carcinoma using anti-EGFR antibody conjugated gold nanoparticles. *Cancer Lett*. 2006;239(1):129–135.
20. Xu S, Hartvickson S, Zhao JX. Increasing surface area of silica nanoparticles with a rough surface. *ACS Appl Mater Interfaces*. 2011; 3(6):1865–1872.
21. Rechendorff K, Hovgaard MB, Foss M, Zhdanov VP, Besenbacher F. Enhancement of protein adsorption induced by surface roughness. *Langmuir*. 2006;22(26):10885–10888.

22. Tsujioka K. [Apparatus engineering of x ray CT equipment (2): image reconstruction and image display]. *Nihon Hoshasen Gijutsu Gakkai Zasshi*. 2002;58(3):355–359. Japanese.

23. Fenton SJ, Hansen KW, Meyers RL, et al. CT scan and the pediatric trauma patient – are we overdoing it? *J Pediatr Surg*. 2004;39(12): 1877–1881.

24. Andersson LE, Bååth M, Thörne A, Aspelin P, Odeberg-Wernerman S. Effect of carbon dioxide pneumoperitoneum on development of atelectasis during anesthesia, examined by spiral computed tomography. *Anesthesiology*. 2005;102(2):293–299.

25. Hainfeld JF, Slatkin DN, Focella TM, Smilowitz HM. Gold nanoparticles: a new X-ray contrast agent. *Br J Radiol*. 2006;79(939):248–253.

26. Kim D, Park S, Lee JH, Jeong YY, Jon S. Antibiofouling polymer-coated gold nanoparticles as a contrast agent for *in vivo* X-ray computed tomography imaging. *J Am Chem Soc*. 2007;129(24):7661–7665.

27. Umair M, Javed I, Rehman M, et al. Nanotoxicity of inert materials: the case of gold, silver and iron. *J Pharm Pharm Sci*. 2016;19(2): 161–180.

28. Pérez SE, Gándola Y, Carlucci AM, González L, Turyn D, Bregni C. Formulation strategies, characterization, and in vitro evaluation of lecithin-based nanoparticles for siRNA delivery. *J Drug Deliv*. 2012;2012:986265.

29. Glazer ES, Zhu C, Hamir AN, Borne A, Thompson CS, Curley SA. Biodistribution and acute toxicity of naked gold nanoparticles in a rabbit hepatic tumor model. *Nanotoxicology*. 2011;5(4):459–468.

30. Sonavane G, Tomoda K, Makino K. Biodistribution of colloidal gold nanoparticles after intravenous administration: effect of particle size. *Colloids Surf B Biointerfaces*. 2008;66(2):274–280.

31. Ivanov MR, Bednar HR, Haes AJ. Investigations of the mechanism of gold nanoparticle stability and surface functionalization in capillary electrophoresis. *ACS Nano*. 2009;3(2):386–394.

32. Clogston JD, Patri AK. Zeta potential measurement. *Methods Mol Biol*. 2011;697:63–70.

33. Jain S, Hirst DG, O'Sullivan JM. Gold nanoparticles as novel agents for cancer therapy. *Br J Radiol*. 2012;85(1010):101–113.

34. Lusic H, Grinstaff MW. X-ray-computed tomography contrast agents. *Chem Rev*. 2013;113(3):1641–1666.

35. Bednarski M, Dudek M, Knutelska J, et al. The influence of the route of administration of gold nanoparticles on their tissue distribution and basic biochemical parameters: in vivo studies. *Pharmacol Rep*. 2015;67(3): 405–409.